

Electrical conductivity of hot relativistic plasma in a strong magnetic field

Ritesh Ghosh^{1,*} and Igor A. Shovkovy^{1,2,†}

¹*College of Integrative Sciences and Arts, Arizona State University, Mesa, Arizona 85212, USA*

²*Department of Physics, Arizona State University, Tempe, Arizona 85287, USA*

(Dated: April 1, 2024)

We employ first-principles quantum field theoretical methods to investigate the longitudinal and transverse electrical conductivities of a strongly magnetized hot QED plasma at the leading order in coupling. The analysis utilized the fermion damping rate in the Landau-level representation obtained recently. In the relativistic regime, both conductivities exhibit a scaling behavior given by $\sigma_{\parallel,\perp} = T\tilde{\sigma}_{\parallel,\perp}$, where $\tilde{\sigma}_{\parallel,\perp}$ are functions of the dimensionless ratio $|eB|/T^2$ (here T denotes the temperature and B the magnetic field). As $|eB|/T^2$ increases, both conductivities initially decrease, reach minima, and then exhibit growths when the lowest Landau level dominates. However, the mechanisms for the transverse and longitudinal conductivities differ significantly, leading to a strong suppression of the former in comparison to the latter. Additionally, we extend our analysis to a magnetized quark-gluon plasma, although the approximation's validity breaks down in QCD at strong coupling.

Introduction. Relativistic plasmas are common in cosmology, astrophysics, and heavy-ion collisions. In many cases, they coexists with strong magnetic fields [1–4]. To understand the physical properties of such plasmas, one often needs to know their transport properties. One such defining property is electrical conductivity. It affects the decay (production) rate of magnetic fields, diffusion of charge fluctuations, and even the absorption (emission) of low-energy electromagnetic probes.

In the absence of background magnetic fields, the electrical conductivity of a relativistic QED plasma has been investigated by many authors [5–9]. To some extent, it was also studied in weak magnetic fields [10, 11]. However, there are no rigorous calculations of the electrical conductivity in strongly magnetized plasmas when the Landau-level quantization becomes important. Note, however, that some attempts have been undertaken in the context of quark-gluon plasma (QGP) using analytical methods [12, 13] and lattice calculations [14–17]. Here we address the problem from first principles in a weakly coupled plasma in a quantizing magnetic field. (We will also make an attempt to extrapolate the results to strongly coupled QGP, although it is formally outside the validity range of the approximations used.)

The common technique for calculating electrical conductivity is kinetic theory. However, it is inapplicable in quantizing magnetic fields when quantum states ψ_n of charged particles are labeled by discrete Landau levels, $n = 0, 1, 2, \dots$, rather than continuous transverse momenta. In this case, one must use methods of quantum field theory to calculate transport properties. This is the approach we utilize in the current study to obtain electrical conductivity in a hot strongly magnetized QED plasma. We concentrate primarily on the electron-positron plasma in an ultra-relativistic regime with $\sqrt{|eB|} \gtrsim T \gg m_e$. However, the method is also valid at lower temperatures and weaker magnetic fields, provided $\sqrt{|eB|} \gtrsim T$ [18].

Formalism. Electrical conductivity is a measure of how easily current flows in response to an applied electric field. At the microscopic level, it is determined by the damping rate (or the quasiparticle width) of charge carriers in the plasma. Generally, the smaller the damping rates of particles (which correlate with longer mean free paths), the greater the conductivity. In a strong magnetic field, this remains true for the longitudinal but not the transverse conductivity. Indeed, the magnetic field constrains the movement of charge carriers in perpendicular directions, resulting in a significant suppression of transport. As we explain below, it is the interactions responsible for particle damping that actually facilitate the flow of the transverse electrical current.

The fermion damping rate in a hot, strongly magnetized relativistic plasma has recently been calculated at the leading order in coupling [19]. The resulting rate $\Gamma_n(k_z)$ depends on both the Landau-level index n and the longitudinal momentum k_z . In the presence of a sufficiently strong magnetic field, $\Gamma_n(k_z)$ is determined by the one-to-two and two-to-one processes: $\psi_n \rightarrow \psi_{n'} + \gamma$, $\psi_n + \gamma \rightarrow \psi_{n'}$, and $\psi_n + \bar{\psi}_{n'} \rightarrow \gamma$, where γ is a photon. In the absence of a magnetic field, these processes are forbidden due to the energy-momentum conservation. Consequently, in the weak field limit, the sub-leading two-to-two processes, $\psi_n + \gamma \rightarrow \psi_{n'} + \gamma$ and $\psi_n + \bar{\psi}_{n'} \rightarrow \gamma + \gamma$, must dominate. Roughly estimated, the magnitude of the leading-order contributions is $\alpha|eB|/T$, while the sub-leading processes are of the order $\alpha^2 T$, where $\alpha = 1/137$ is the fine structure constant. In the rest of this study, therefore, we will assume that $|eB|/T^2 \gg \alpha$.

To calculate the electrical conductivity tensor σ_{ij} , we will use the Kubo linear-response theory. It relates the corresponding transport characteristics to the imaginary part of the polarization tensor, i.e.,

$$\sigma_{ij} = \lim_{\Omega \rightarrow 0} \frac{\text{Im} \Pi_{ij}(\Omega + i0; \mathbf{0})}{\Omega}. \quad (1)$$

At one-loop order, the momentum-space expression for the polarization tensor is given by

$$\Pi_{ij}(\Omega; \mathbf{0}) = 4\pi\alpha \oint_{\mathbf{k}} \text{tr} \left[\gamma^i \bar{G}(i\omega_{\mathbf{k}}; \mathbf{k}) \gamma^j \bar{G}(i\omega_{\mathbf{k}} - \Omega; \mathbf{k}) \right], \quad (2)$$

where $\bar{G}(i\omega_{\mathbf{k}}; \mathbf{k})$ is the Fourier transform of the translation invariant part of the fermion propagator [4], $\omega_{\mathbf{k}} = \pi T(2k + 1)$ is the fermion Matsubara frequency, and $\oint_{\mathbf{k}} \equiv T \sum_{k=-\infty}^{\infty} \int d^3\mathbf{k}/(2\pi)^3$.

It is convenient to use the following spectral representation for the fermion propagator:

$$\bar{G}(i\omega_{\mathbf{k}}; \mathbf{k}) = \int_{-\infty}^{\infty} \frac{dk_0 A_{\mathbf{k}}(k_0)}{i\omega_{\mathbf{k}} - k_0 + \mu}. \quad (3)$$

Assuming that the electrical charge chemical potential μ is zero, the off-diagonal components of conductivity vanish. The remaining diagonal components are given by the following expression [20]:

$$\sigma_{ii} = -\frac{\alpha}{8\pi T} \int \int \frac{dk_0 d^3\mathbf{k}}{\cosh^2 \frac{k_0}{2T}} \text{tr} \left[\gamma^i A_{\mathbf{k}}(k_0) \gamma^i A_{\mathbf{k}}(k_0) \right]. \quad (4)$$

$$\sigma_{\perp} \simeq \frac{\alpha}{\pi \ell^2 T} \sum_{n=0}^{\infty} \int_0^{\infty} \frac{dk_z (\Gamma_n + \Gamma_{n+1}) \left[2(2n+1)|eB| + (\Gamma_n + \Gamma_{n+1})^2 \right]}{\left[(E_n - E_{n+1})^2 + (\Gamma_n + \Gamma_{n+1})^2 \right] \left[(E_n + E_{n+1})^2 + (\Gamma_n + \Gamma_{n+1})^2 \right]} \left(\frac{1}{\cosh^2 \frac{E_n}{2T}} + \frac{1}{\cosh^2 \frac{E_{n+1}}{2T}} \right), \quad (6)$$

and

$$\sigma_{\parallel} \simeq \frac{\alpha}{2\pi \ell^2 T} \sum_{n=0}^{\infty} \beta_n \int_0^{\infty} \frac{dk_z (k_z^2 + \Gamma_n^2)}{\Gamma_n (E_n^2 + \Gamma_n^2) \cosh^2 \frac{E_n}{2T}}, \quad (7)$$

respectively. In the last expression, we used $\beta_n \equiv 2 - \delta_{n,0}$.

The longitudinal conductivity in Eq. (7) is determined by a sum of contributions from individual Landau levels. The corresponding states can be formally viewed as distinct species of particles. As usual, each of them contributes proportionally to the inverse damping rate: $\sigma_{\parallel} = \sum_n \sigma_{\parallel,n}$, where $\sigma_{\parallel,n} \propto 1/\Gamma_n$.

In contrast, the nature of transverse conductivity differs substantially. The partial contributions in Eq. (6) are proportional to the damping rates rather than their inverse values, i.e., $\sigma_{\perp} = \sum_n \sigma_{\perp,n}$, where $\sigma_{\perp,n} \propto \Gamma_n + \Gamma_{n+1}$. This reflects a unique conduction regime with the magnetic field confining charged particles in the transverse plane, but interactions providing a transport pathway through quantum “jumps” between Landau levels.

Electrical conductivity in QED plasma. The formal expressions for the transverse and longitudinal conductivities in Eqs. (6) and (7) are only as good as the quality of input about the fermion damping rates $\Gamma_n(k_z)$. Here we rely on the recent results for the Landau-level dependent damping rates obtained at the leading order in coupling in Ref. [19]. Because of weak coupling, the corresponding approximation should be reliable in the case

In this representation, the spectral density $A_{\mathbf{k}}(k_0)$ contains all essential information about the damping rate of charge carriers $\Gamma_n(k_z)$. The explicit expression of $A_{\mathbf{k}}(k_0)$ reads

$$A_{\mathbf{k}}(k_0) = \frac{ie^{-k_{\perp}^2 \ell^2}}{\pi} \sum_{\lambda=\pm} \sum_{n=0}^{\infty} \frac{(-1)^n}{E_n} \left\{ [E_n \gamma^0 - \lambda k_z \gamma^3 + \lambda m_e] \times [\mathcal{P}_+ L_n(2k_{\perp}^2 \ell^2) - \mathcal{P}_- L_{n-1}(2k_{\perp}^2 \ell^2)] + 2\lambda(\mathbf{k}_{\perp} \cdot \boldsymbol{\gamma}_{\perp}) L_{n-1}^1(2k_{\perp}^2 \ell^2) \right\} \frac{\Gamma_n}{(k_0 - \lambda E_n)^2 + \Gamma_n^2} \quad (5)$$

where $\ell = 1/\sqrt{|eB|}$ is the magnetic length, $E_n = \sqrt{2n|eB| + m_e^2 + k_z^2}$ is the Landau-level energy, $\mathcal{P}_{\pm} = (1 \mp i\gamma^1 \gamma^2)/2$ are the spin projectors, and $L_n^{\alpha}(z)$ are the generalized Laguerre polynomials [21]. To simplify the notation, we suppressed the explicit dependence of E_n and Γ_n on the longitudinal momentum k_z .

Substituting spectral density (5) into Eq. (4), and integrating over \mathbf{k}_{\perp} , we derive the final expressions for the transverse and longitudinal conductivities, i.e.,

of QED plasma, assuming $|eB|/T^2 \gg \alpha$.

To calculate electrical conductivities, we begin by generating numerical data for the damping rates across a wide range of magnetic fields (from $|eB| = 225m_e^2$ to $|eB| = 25600m_e^2$) and temperatures (from $T = 10m_e$ to $T = 80m_e$). Following the methodology outlined in Ref. [19], we compute $\Gamma_n(k_z)$ for all Landau levels up to $n = 50$. In our calculation, however, we account for all processes involving Landau-level states with indices up to $n_{\max} = 100$. Such a large phase space enables us to attain a good approximation in plasmas with $|eB|/T^2 \gtrsim 0.1$, covering the entire range of validity of the leading-order approximation.

Using the numerical data for damping rates $\Gamma_n(k_z)$, we then readily calculate the transverse and longitudinal conductivities, defined by Eqs. (6) and (7), respectively. The results are summarized in Fig. 1, where we show the dimensionless ratios $\tilde{\sigma}_{\perp} \equiv \sigma_{\perp}/T$ (orange) and $\tilde{\sigma}_{\parallel} \equiv \sigma_{\parallel}/T$ (blue) as functions of $|eB|/T^2$. (For the numerical data, see Supplementary Materials [22].)

As we see, despite a wide range of magnetic fields and temperatures, nearly all data fall on the same curve. This is not surprising since the effects of a nonzero fermion mass are negligible in the ultrarelativistic regime with $\sqrt{|eB|/T} \gg m_e$ and $T \gg m_e$. In such a scaling regime, $|eB|/T^2$ is the only relevant dimensionless parameter that

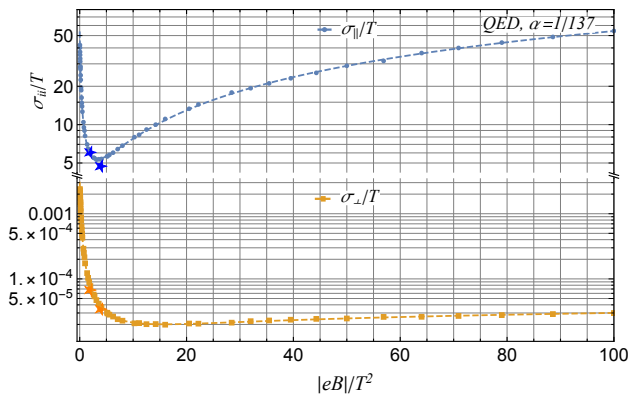


FIG. 1. The longitudinal and transverse conductivities in QED. The dashed lines represent the analytical fits in Eqs. (8) and (9). Two extra points (labeled by stars) correspond to a low temperature, $T = 2.5m_e$, and two relatively weak magnetic fields, $|eB| = 12.5m_e^2$ and $|eB| = 25m_e^2$.

determines $\tilde{\sigma}_{\perp}$ and $\tilde{\sigma}_{\parallel}$.

Of course, deviations from the universal scaling dependence in Fig. 1 become noticeable with decreasing of the temperature and/or the magnetic field. To demonstrate this, we included two such cases in Fig. 1, labeled by stars. They represent conductivities at a relatively low temperature, $T = 2.5m_e \approx 1.28$ MeV, and two rather weak magnetic fields, $|eB| = 12.5m_e^2$ ($B \approx 5.52 \times 10^{14}$ G) and $|eB| = 25m_e^2$ ($B \approx 1.10 \times 10^{15}$ G).

In the scaling regime, the transverse and longitudinal conductivities can be fitted by the following Padé approximants:

$$\frac{\tilde{\sigma}_{\perp}^{\text{QED}}}{\tilde{\sigma}_{\perp,0}} = \frac{1 + 0.517b + 0.045b^2 + 0.0058b^3 + 9.7 \times 10^{-6}b^4}{1 + 7.68b + 17.9b^2 + 0.0585b^3} \quad (8)$$

$$\frac{\tilde{\sigma}_{\parallel}^{\text{QED}}}{\tilde{\sigma}_{\parallel,0}} = \frac{1 + 0.213b + 0.0784b^2 + 3.4 \times 10^{-5}b^3}{1 + 7.31b + 0.00888b^2}, \quad (9)$$

where $\tilde{\sigma}_{\perp,0} \approx 0.00316$, $\tilde{\sigma}_{\parallel,0} \approx 53.0$, and $b = |eB|/T^2$. In the whole range with $0.1 \lesssim |eB|/T^2 \lesssim 256$, the quality of the fit is better than about 5% for $\tilde{\sigma}_{\perp}$ and 2% for $\tilde{\sigma}_{\parallel}$.

In accordance with the very different underlying mechanisms mentioned earlier, the values of $\tilde{\sigma}_{\perp}$ and $\tilde{\sigma}_{\parallel}$ differ by about 5 to 7 orders of magnitude in QED. This is consistent with a qualitative dependence on the coupling constant, provided $\sigma_{\perp} \propto \Gamma_n \propto \alpha$ and $\sigma_{\parallel} \propto 1/\Gamma_n \propto 1/\alpha$.

As $|eB|/T^2$ increases, both conductivities initially decrease, reach minima, and then grow. The decrease of $\tilde{\sigma}_{\parallel}$ at small b comes from a gradual reduction of the Landau-level phase space contributing to transport and, in part, from the damping rates $\Gamma_n(k_z)$ increasing with the field. In the case of $\tilde{\sigma}_{\perp}$, the reduction of the phase space is further enhanced by the effect of magnetic field trapping. The growth of $\Gamma_n(k_z)$ with the field becomes important only at much higher values of b , where conduction is governed mostly by the lowest Landau level. The conductivities are approximately linear at large b , which could be

explained by the density of states in the lowest Landau level $\propto |eB|$.

Electrical conductivity of QGP. QGP is another variant of relativistic plasma, which can be created in ultrarelativistic heavy-ion collisions. The electrical conductivity plays an important role in heavy-ion phenomenology [23–26]. It determines the relaxation time of the background magnetic field and, in turn, affects various observable signatures linked with the chiral magnetic effect and other phenomena. (For reviews, see Refs. [3, 4].)

There have been many attempts in the literature to study the effect of a magnetic field on the electrical conductivity of QGP. The methods ranged from various versions of kinetic theory [13, 27–30] to field theory models [12, 31–33], holographic QCD [34, 35], and lattice QCD [17, 36].

In contrast to its QED counterpart, QGP is made of strongly interacting quarks and gluons, rendering perturbative techniques generally inapplicable. However, by invoking the principles of asymptotic freedom [37, 38], one can argue that such a plasma becomes weakly interacting at extremely high temperatures [39] and/or under superstrong magnetic fields [40]. Then, one can use perturbative methods to illuminate transport properties of QGP. Building upon these general, albeit simplistic, arguments, we extend our field-theoretical calculations of electrical conductivity to a strongly magnetized QGP.

Here we will assume that a hot QCD plasma is made of the lightest up and down quarks (each coming in three colors, $N_c = 3$). For simplicity, we will assign the same current masses to both flavors, $m = 5$ MeV. However, we will account for their different electrical charges, $q_u = 2e/3$ and $q_d = -e/3$, which affect their interaction with the background magnetic field.

The contributions of the two quark flavors to the transverse and longitudinal conductivities are given by expressions similar to those in Eqs. (6) and (7). The quark electrical charges and colors are accounted for by replacing α with $\alpha N_c (q_f/e)^2$ and $|eB|$ with $|q_f B|$ ($f = u, d$).

A less apparent but crucial distinction arises also in the damping rates of quarks, $\Gamma_n^f(k_z)$. At the leading order in the strong coupling constant, $\alpha_s = g_s^2/(4\pi)$, these rates are determined by one-to-two and two-to-one processes: $\psi_n \rightarrow \psi_{n'} + g$, $\psi_n + g \rightarrow \psi_{n'}$, and $\psi_n + \bar{\psi}_{n'} \rightarrow g$, where g represents a gluon. These rates are roughly of the order of $\alpha_s |eB|/T$ [19]. Although the value of α_s decreases with increasing the temperature, it is likely to remain on the order of 1 in the QGP created by heavy-ion collisions.

Clearly, the leading-order approximation is inadequate for reliably estimating the electrical conductivity in a strongly interacting regime of QGP. Nevertheless, we will formally extend our calculations to such a regime. Hopefully, these results will offer a valuable qualitative benchmark until more refined nonperturbative field-theoretical approaches are developed.

Our numerical results are compiled in Fig. 2. (See also

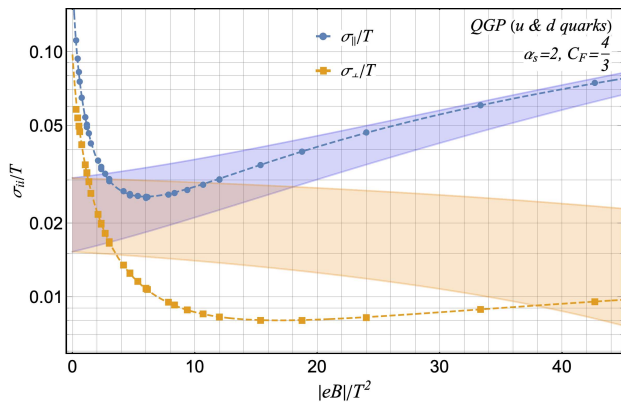


FIG. 2. The longitudinal and transverse conductivities in two-flavor QCD. The dashed lines represent the analytical fits in Eqs. (10) and (11). The blue and orange bands show the approximate ranges of longitudinal and transverse conductivities obtained in lattice QCD [17].

Supplementary Materials [22].) Once again, we show the dimensionless ratios $\tilde{\sigma}_\perp \equiv \sigma_\perp/T$ (orange) and $\tilde{\sigma}_\parallel \equiv \sigma_\parallel/T$ (blue) as functions of $|eB|/T^2$. In an ultrarelativistic plasma, which is well-justified above the QCD deconfinement temperature, $|eB|/T^2$ is the sole dimensionless parameter that determines conductivity in units of temperature. The scaling dependence is supported by numerous data points falling on the same universal curve in Fig. 2. Here, we disregard the running of QCD coupling, which should introduce deviations from the scaling behavior. Interestingly, upon scrutinizing the lattice data in Ref. [17], we revealed nearly perfect scaling dependences for both conductivities.

In calculating the quark damping rates, $\Gamma_n^f(k_z)$, we needed to specify the value of the strong coupling constant α_s . For guidance, we used lattice QCD results [17] to match approximately the increase of $\tilde{\sigma}_\parallel$ with the field, and found that $\alpha_s = 2$ works reasonably well. Clearly, such a large value renders the perturbative approach invalid. Nonetheless, we observe that the conductivity results in Fig. 2 replicate some qualitative features of both transverse and longitudinal conductivities on the lattice, represented by the orange and blue shaded bands. (The upper and lower edges of the bands correspond to $\sigma_0 = 0.3C_{\text{em}}T$ and $\sigma_0 = 0.6C_{\text{em}}T$, where $C_{\text{em}} = 5e^2/9$.)

Our QCD results for the transverse and longitudinal conductivities in Fig. 2 can be fitted by the following Padé approximants:

$$\frac{\tilde{\sigma}_\perp^{\text{QCD}}}{\tilde{\sigma}_{\perp,0}} = \frac{1 + 0.0514b + 0.006423b^2 + 2.47 \times 10^{-5}b^3}{1 + 1.86b + 0.047b^2 + 5.16 \times 10^{-5}b^3} \quad (10)$$

$$\frac{\tilde{\sigma}_\parallel^{\text{QCD}}}{\tilde{\sigma}_{\parallel,0}} = \frac{1 + 0.103b + 0.025b^2 + 3.26 \times 10^{-5}b^3}{1 + 3.059b + 0.0063b^2}, \quad (11)$$

where $\tilde{\sigma}_{\perp,0} \approx 0.0968$, $\tilde{\sigma}_{\parallel,0} \approx 0.199$, and $b = |eB|/T^2$. The quality of these fits are better than about 2% for both

transverse and longitudinal conductivities in the whole range of parameters studied.

Although our leading-order calculations cannot offer any quantitative predictions, they do provide a deeper insight into the electric charge transport in a strongly magnetized QGP. As in QED, the underlying mechanisms responsible for the transverse and longitudinal conductivities are very different in the presence of a strong magnetic field. While the former tends to be enhanced by interactions ($\sigma_{\perp,n} \propto \Gamma_n + \Gamma_{n+1}$), the latter is suppressed by them ($\sigma_{\parallel,n} \propto 1/\Gamma_n$). In principle, this can be verified by using lattice methods in various QCD-like theories with different coupling constants α_s . According to our predictions, the ratio of the transverse to the longitudinal conductivity should scale roughly as α_s^2 .

In connection with the electric conductivity of QGP, it is instructive to compare our results with two earlier studies in Refs. [12, 13], which bare some similarities to our approach. The authors of Ref. [12] employ a method similar to ours but focus only longitudinal transport and utilize a simpler approximation for the fermion damping rates. In Ref. [13], the authors develop a special formulation of kinetic theory for longitudinal transport in a strong magnetic field. While the shape of their scaling function $\tilde{\sigma}_\parallel$ resemble ours, it differs significantly in magnitude and detail. Also, the method of Ref. [13] cannot be applied to transverse transport.

Summary. In this study, we used first-principles quantum-field theoretical methods to calculate the electrical conductivity of strongly magnetized hot relativistic plasmas. Our calculation relies on the Kubo formula and utilizes leading-order results for the Landau-level dependent fermion damping rates $\Gamma_n(p_z)$. For calculating $\Gamma_n(p_z)$, we utilized the formalism developed recently in Ref. [19]. In a sufficiently strong magnetic field, the damping rates are dominated by the one-to-two and two-to-one processes: $\psi_n \rightarrow \psi_{n'} + \gamma$, $\psi_n + \gamma \rightarrow \psi_{n'}$, and $\psi_n + \bar{\psi}_{n'} \rightarrow \gamma$. The corresponding leading-order analysis is claimed to be valid when the magnetic field and temperature satisfy the inequality $|eB|/T^2 \gg \alpha$. For smaller ratios, the approximation breaks down because the damping rates are dominated by the sub-leading two-to-two processes, $\psi_n + \gamma \rightarrow \psi_{n'} + \gamma$ and $\psi_n + \bar{\psi}_{n'} \rightarrow \gamma + \gamma$.

For simplicity, here we concentrated primarily on ultrarelativistic plasmas, which are realized when $T \gg m_e$ and $\sqrt{|eB|} \gg m_e$. In this regime, the ratios of the longitudinal and transverse conductivities to the temperature, σ_\perp/T and σ_\parallel/T , are given by universal scaling functions $\tilde{\sigma}_\perp$ and $\tilde{\sigma}_\parallel$ that depend only on $|eB|/T^2$. For a QED plasma, the corresponding numerical results are presented in Fig. 1.

As expected, electric charge transport reveals a high degree of anisotropy in a strong magnetic field. In the case of QED, the values of $\tilde{\sigma}_\perp$ are 5 to 7 orders of magnitudes smaller than $\tilde{\sigma}_\parallel$. More importantly, the underlying mechanisms for transport differ significantly in the transverse and longitudinal directions. Without interactions,

the motion of charge carriers is unimpeded in the direction parallel to the magnetic field but highly restricted in the perpendicular directions. The effect of interactions is opposite. While particle scattering into other states suppresses longitudinal transport, transitions between different Landau-level orbitals facilitate transverse transport. Consequently, the longitudinal conductivity scales with the coupling constant as $1/\alpha$, but the transverse conductivity scales as α , resulting in a huge difference between the two.

Considering the phenomenological importance of electrical conductivity in heavy-ion physics, we tried to extrapolate our leading-order calculations to the case of strongly magnetized QGP. To get the same orders of magnitude for the electrical conductivities as in lattice QCD [17], we had to choose a rather large value of the strong coupling constant, $\alpha_s = 2$. Clearly, the leading-order approximation breaks down at such large coupling. Only non-perturbative techniques have a chance to provide reliable quantitative results in this regime. Nonetheless, our simplistic analysis might be valuable to understand qualitative differences between longitudinal and transverse transport in the strongly magnetized QGP.

This research was funded in part by the U.S. National Science Foundation under Grant No. PHY-2209470.

* Ritesh.Ghosh@asu.edu

† Igor.Shovkovy@asu.edu

- [1] D. Grasso and H. R. Rubinstein, Magnetic fields in the early universe, *Phys. Rept.* **348**, 163 (2001), [arXiv:astro-ph/0009061](#).
- [2] D. Price and S. Rosswog, Producing ultra-strong magnetic fields in neutron star mergers, *Science* **312**, 719 (2006), [arXiv:astro-ph/0603845](#).
- [3] D. E. Kharzeev, J. Liao, S. A. Voloshin, and G. Wang, Chiral magnetic and vortical effects in high-energy nuclear collisions—A status report, *Prog. Part. Nucl. Phys.* **88**, 1 (2016), [arXiv:1511.04050](#).
- [4] V. A. Miransky and I. A. Shovkovy, Quantum field theory in a magnetic field: From quantum chromodynamics to graphene and Dirac semimetals, *Phys. Rept.* **576**, 1 (2015), [arXiv:1503.00732](#).
- [5] J. Ahonen and K. Enqvist, Electrical conductivity in the early universe, *Phys. Lett. B* **382**, 40 (1996), [arXiv:hep-ph/9602357](#).
- [6] G. Baym and H. Heiselberg, The Electrical conductivity in the early universe, *Phys. Rev. D* **56**, 5254 (1997), [arXiv:astro-ph/9704214](#).
- [7] P. B. Arnold, G. D. Moore, and L. G. Yaffe, Transport coefficients in high temperature gauge theories. 1. Leading log results, *JHEP* **11**, 001, [arXiv:hep-ph/0010177](#).
- [8] D. Boyanovsky, H. J. de Vega, and S.-Y. Wang, Dynamical renormalization group approach to transport in ultra-relativistic plasmas: The Electrical conductivity in high temperature QED, *Phys. Rev. D* **67**, 065022 (2003), [arXiv:hep-ph/0212107](#).
- [9] P. B. Arnold, G. D. Moore, and L. G. Yaffe, Transport coefficients in high temperature gauge theories. 2. Beyond leading log, *JHEP* **05**, 051, [arXiv:hep-ph/0302165](#).
- [10] H. van Erkelens and W. van Leeuwen, Relativistic boltzmann theory for a plasma: X. electrical conduction of the cosmological fluid, *Physica A* **123**, 72 (1984).
- [11] O. J. Pike and S. J. Rose, Transport coefficients of a relativistic plasma, *Phys. Rev. E* **93**, 053208 (2016).
- [12] K. Hattori and D. Satow, Electrical Conductivity of Quark-Gluon Plasma in Strong Magnetic Fields, *Phys. Rev. D* **94**, 114032 (2016), [arXiv:1610.06818 \[hep-ph\]](#).
- [13] K. Fukushima and Y. Hidaka, Electric conductivity of hot and dense quark matter in a magnetic field with Landau level resummation via kinetic equations, *Phys. Rev. Lett.* **120**, 162301 (2018), [arXiv:1711.01472 \[hep-ph\]](#).
- [14] G. Aarts, C. Allton, A. Amato, P. Giudice, S. Hands, and J. Skullerud, Electrical conductivity and charge diffusion in thermal QCD from the lattice, *JHEP* **02**, 186, [arXiv:1412.6411](#).
- [15] B. B. Brandt, A. Francis, B. Jäger, and H. B. Meyer, Charge transport and vector meson dissociation across the thermal phase transition in lattice QCD with two light quark flavors, *Phys. Rev. D* **93**, 054510 (2016), [arXiv:1512.07249 \[hep-lat\]](#).
- [16] H.-T. Ding, O. Kaczmarek, and F. Meyer, Thermal dilepton rates and electrical conductivity of the QGP from the lattice, *Phys. Rev. D* **94**, 034504 (2016), [arXiv:1604.06712 \[hep-lat\]](#).
- [17] N. Astrakhantsev, V. V. Braguta, M. D’Elia, A. Y. Kotov, A. A. Nikolaev, and F. Sanfilippo, Lattice study of the electromagnetic conductivity of the quark-gluon plasma in an external magnetic field, *Phys. Rev. D* **102**, 054516 (2020), [arXiv:1910.08516 \[hep-lat\]](#).
- [18] R. Ghosh and I. A. Shovkovy, Anisotropic charge transport in strongly magnetized relativistic matter, (2024), in preparation.
- [19] R. Ghosh and I. A. Shovkovy, The fermion self-energy and damping rate in a hot magnetized plasma, (2024), [arXiv:2402.04307 \[hep-ph\]](#).
- [20] E. Gorbar, V. Miransky, and I. Shovkovy, Chiral anomaly, dimensional reduction, and magnetoresistivity of Weyl and Dirac semimetals, *Phys. Rev.* **B89**, 085126 (2014), [arXiv:1312.0027](#).
- [21] I. S. Gradshteyn and I. M. Ryzhik, *New York: Academic Press, 1980, 5th corr. and enl. ed.* (Academic Press, Orlando, 1980).
- [22] R. Ghosh and I. A. Shovkovy, Data files for electrical conductivity of hot relativistic plasma in a strong magnetic field, <https://www.dropbox.com/scl/fo/74k911n0simacisc4wydg/h?rlke> (2024).
- [23] K. Tuchin, Time and space dependence of the electromagnetic field in relativistic heavy-ion collisions, *Phys. Rev. C* **88**, 024911 (2013), [arXiv:1305.5806 \[hep-ph\]](#).
- [24] L. McLerran and V. Skokov, Comments About the Electromagnetic Field in Heavy-Ion Collisions, *Nucl. Phys. A* **929**, 184 (2014), [arXiv:1305.0774 \[hep-ph\]](#).
- [25] U. Gursoy, D. Kharzeev, and K. Rajagopal, Magneto-hydrodynamics, charged currents and directed flow in heavy ion collisions, *Phys. Rev. C* **89**, 054905 (2014),

- arXiv:1401.3805 [hep-ph].
- [26] K. Tuchin, Initial value problem for magnetic fields in heavy ion collisions, *Phys. Rev. C* **93**, 014905 (2016), arXiv:1508.06925 [hep-ph].
- [27] A. Bandyopadhyay, S. Ghosh, R. L. S. Farias, J. Dey, and G. a. Krein, Anisotropic electrical conductivity of magnetized hot quark matter, *Phys. Rev. D* **102**, 114015 (2020), arXiv:1911.10005 [hep-ph].
- [28] J. Dey, S. Satapathy, P. Murmu, and S. Ghosh, Shear viscosity and electrical conductivity of the relativistic fluid in the presence of a magnetic field: A massless case, *Pramana* **95**, 125 (2021), arXiv:1907.11164 [hep-ph].
- [29] J. Dey, S. Satapathy, A. Mishra, S. Paul, and S. Ghosh, From noninteracting to interacting picture of quark-gluon plasma in the presence of a magnetic field and its fluid property, *Int. J. Mod. Phys. E* **30**, 2150044 (2021), arXiv:1908.04335 [hep-ph].
- [30] A. Das, H. Mishra, and R. K. Mohapatra, Electrical conductivity and Hall conductivity of a hot and dense quark gluon plasma in a magnetic field: A quasi-particle approach, *Phys. Rev. D* **101**, 034027 (2020), arXiv:1907.05298 [hep-ph].
- [31] S. Satapathy, S. Ghosh, and S. Ghosh, Kubo estimation of the electrical conductivity for a hot relativistic fluid in the presence of a magnetic field, *Phys. Rev. D* **104**, 056030 (2021), arXiv:2104.03917 [hep-ph].
- [32] H.-H. Peng, X.-L. Sheng, S. Pu, and Q. Wang, Electric and magnetic conductivities in magnetized fermion systems, *Phys. Rev. D* **107**, 116006 (2023), arXiv:2304.00519 [nucl-th].
- [33] A. Bandyopadhyay, S. Ghosh, R. L. S. Farias, and S. Ghosh, Quantum version of transport coefficients in Nambu–Jona-Lasinio model at finite temperature and strong magnetic field, *Eur. Phys. J. C* **83**, 489 (2023), arXiv:2305.15844 [hep-ph].
- [34] K. Fukushima and A. Okutsu, Electric conductivity with the magnetic field and the chiral anomaly in a holographic QCD model, *Phys. Rev. D* **105**, 054016 (2022), arXiv:2106.07968 [hep-ph].
- [35] W. Li, S. Lin, and J. Mei, Conductivities of magnetic quark-gluon plasma at strong coupling, *Phys. Rev. D* **98**, 114014 (2018), arXiv:1809.02178 [hep-th].
- [36] P. V. Buividovich, M. N. Chernodub, D. E. Kharzeev, T. Kalaydzhyan, E. V. Luschevskaya, *et al.*, Magnetic-Field-Induced insulator-conductor transition in SU(2) quenched lattice gauge theory, *Phys. Rev. Lett.* **105**, 132001 (2010), arXiv:1003.2180.
- [37] D. J. Gross and F. Wilczek, Ultraviolet Behavior of Nonabelian Gauge Theories, *Phys. Rev. Lett.* **30**, 1343 (1973).
- [38] H. D. Politzer, Reliable Perturbative Results for Strong Interactions?, *Phys. Rev. Lett.* **30**, 1346 (1973).
- [39] W. Busza, K. Rajagopal, and W. van der Schee, Heavy Ion Collisions: The Big Picture, and the Big Questions, *Ann. Rev. Nucl. Part. Sci.* **68**, 339 (2018), arXiv:1802.04801 [hep-ph].
- [40] V. A. Miransky and I. A. Shovkovy, Magnetic catalysis and anisotropic confinement in QCD, *Phys. Rev.* **D66**, 045006 (2002), arXiv:hep-ph/0205348.